Available online at www.sciencedirect.com
ScienceDirect
Journal of Power Sources 161 (2006) 1275–1280
JOURNAL OF POWER SOURCES
www.elsevier.com/locate/jpowsour

# TG-MS analysis of solid electrolyte interphase (SEI) on graphite negative-electrode in lithium-ion batteries

Liwei Zhao *, Izumi Watanabe, Takayuki Doi, Shigeto Okada, Jun-ichi Yamaki

*Institute for Materials Chemistry and Engineering, Kyushu University, Kasuga Koen 6-1, Kasuga 816-8580, Japan*

Received 28 March 2006; received in revised form 25 May 2006; accepted 29 May 2006
Available online 12 July 2006

**Abstract**

The thermal stability and chemical structure of solid electrolyte interphase (SEI) formed on a natural-graphite negative-electrode in ethylene carbonate (EC) and dimethyl carbonate (DMC)-based electrolyte was investigated by thermogravimetry-differential thermal analysis combined with mass spectrometry (TG-DTA/MS) and X-ray photoemission spectroscopy (XPS). Due to the decomposition of SEI, two $CO_2$ evolution peaks at around 330 and 430 °C were detected in TG-MS studies with continuous $CO_2$ background. The continuous $CO_2$ background was attributed to the gradual decomposition of oxygen-containing polymeric species of SEI. Another two dominant components of SEI, lithium alkyl carbonate and lithium oxalate, were found to contribute to the $CO_2$ peaks at 330 and 430 °C separately. The effects of charging-depth, current density and cycle number on the $CO_2$ distribution and XPS spectra were studied. It was found that lithium oxalate was reduction product of lithium alkyl carbonate during the intercalation of lithium ions. The reduction reaction could be accelerated by elevated temperature. The transformation of SEI chemical structure showed direct effect on the thermal stability of SEI. At the same time, lithium carbonate was also found in SEI on the graphite electrode after long cycles, while it was negligible in the electrode subjected to short cycles.


*Keywords:* Lithium-ion battery; Graphite negative-electrode; Solid electrolyte interphase; Thermal analysis

## 1. Introduction

Due to their high energy densities, lithium-ion batteries have been considered as possible power sources in electric vehicles and hybrid electric vehicles. However, before lithium-ion batteries can be used in high-power applications, their performance still needs to be improved with regard to battery cycle life, rate capability, and safety.

In commercially available lithium-ion batteries, graphitic carbon has been generally used as the active material for a negative-electrode due to an acceptably high capacity density, high reversibility and a flat potential close to that of lithium metal [1]. At such a potential, most conventional electrolyte solutions should be thermodynamically unstable. In fact, considerable experimental evidence supports the notion that electrolytes are reductively decomposed to form solid electrolyte interphase (SEI) on graphite, particularly during the initial charging [2,3]. It is generally accepted that the SEI acts as a passivating surface film, and the reversible electrode reaction can proceed even after prolonged charge and discharge cycles. Hence, electrochemical and thermal stabilities of SEI are essential to achieve safe and secure batteries. A mixture of EC and DMC can be used as solvent since an electrochemically stable SEI can be formed on the graphite electrode upon reduction. The chemical composition of SEI has been extensively studied, and it has been reported that SEI should be composed of the reduction products of organic solvents and lithium salts in the electrolytes [2,4–6]. Aurbach et al. [7] investigated the surface reactions at a graphite electrode in EC-based electrolytes. According to their work, the main components of SEI are lithium alkyl carbonate and lithium carbonate. Peled et al. [8] analyzed the SEI on a graphite electrode, and reported that SEI on the edge plane is rich in inorganic compounds, while that precipitated on the basal plane is rich in organic compounds. Zhuang and Ross [9] investigated the SEI on a graphite electrode by Fourier transform infrared spectroscopy using attenuated total reflection (FT-IR-ATR) after aging the cell at a 60% state of charge. They suggested that lithium oxalate, lithium carboxylates and lithium methoxide

* Corresponding author. Tel.: +81 92 583 7657; fax: +81 92 583 7791.
*E-mail address:* zhaolw@cm.kyushu-u.ac.jp (L. Zhao).

0378-7753/$ – see front matter © 2006 Elsevier B.V. All rights reserved.
doi:10.1016/j.jpowsour.2006.05.045

were components of SEI. Furthermore, SEI formed on a graphite electrode has been analyzed by a variety of tools, such as electrochemical impedance spectroscopy (EIS) [10], XPS [11,12], FT-IR [13,14] and scanning electron microscopy (SEM) [15]. However, most of these studies were carried out at room temperature.

In the present work, the thermal stability of SEI was studied by TG-DTA/MS. In addition, the components of SEI were investigated by XPS. The influence of the electrode potential on the thermal stability of SEI will be discussed.

## 2. Experimental

Natural graphite powder (LF-18D, Chuestu Graphite) was used as the active material for a test electrode. The graphite powder (95 wt%) was mixed with a poly(vinylidenefluoride) binder (PVdF, KF#9100, Kureha Chemical) (5 wt%) and dissolved in 1-methyl-2-pyrrolidinone. The slurry was coated on a porous Cu current collector with a thickness of 0.1 mm, and then dried at 120 °C for 12 h in a vacuum oven. The typical loading of the graphite powder was 6 mg $cm^{-2}$.

The electrochemical properties of the graphite were studied by charge/discharge measurements using a two-electrode cell. The graphite test electrode has a round shape with a diameter of 15 mm. A lithium-foil and a polypropylene film (Celgard 3501) were used as the counter electrode and separator, respectively. The electrolyte used was 1 mol $dm^{-3}$ $LiPF_6$ dissolved in a mixture of EC and DMC (1:1, v/v, Tomiyama Chemical). Unless otherwise stated, the charge/discharge cycles were carried out at a constant current rate of 0.2 mA $cm^{-2}$ with a relaxation period of 60 min at the end of each discharge/charge measurement. The charging processes ended at a given potential between 10 mV and 2.0 V, whereas discharging ceased at 2.0 V. After the charge/discharge cycles, the cells were disassembled in an Ar-filled glove box. The test electrode was rinsed and soaked with DMC for 8 h, and then dried under vacuum at room temperature for 10 h to remove low-molecular weight compounds. All of the experiments so far were conducted under an argon atmosphere with a dew point below −80 °C.

The thermal properties of the test electrode were investigated by a Rigaku 8210H/5050AW TG-DTA/MS system (Rigaku, Japan). Sample powders on the test electrode were scraped from the Cu current collector in a glove box. The sample was set in a stainless steel pan to be introduced into the furnace of the TG-DTA, and then heated to 550 °C at a rate of 5 °C $min^{-1}$ under helium flow. Alumina powders were used as reference materials. Gaseous products formed by pyrolysis were identified with a mass spectrometer. The ionization for MS was carried out by electron impact (EI) in which the voltage and the current for acceleration were set at 70 eV and 60 μA, respectively.

The chemical composition of SEI was investigated by XPS using JPS-9010MC/IV (JEOL) with a monochromatic Mg Kα radiation (1253.6 eV). The test electrode was sealed under an argon atmosphere using a vessel for transfer into the XPS sample chamber without being exposed to air. C 1s spectra were obtained by repeated scans (more than 10 times) using a pass-energy of 10 eV. The peak positions were calibrated by reference to an Au 4f level of 84.0 eV with an accuracy of ±0.2 eV.

## 3. Results and discussion

TG-DTA/MS curves of sample powders in the discharged state after the second cycle are shown in Fig. 1. The variation of total ion current (TIC) with temperature is shown together with a mass signal of $m/z = 44$. The sample weight decreased to around 98 wt% below 180 °C, followed by a further decrease to 95 wt% from 200 to 500 °C. The weight at 550 °C was from 95 to 97 wt% regardless of the electrode used. These results suggest that the weight loss was closely related to the thin SEI formed on the graphite electrode. Thus, all of the signals in the curves should be attributed to SEI on the graphite. The DTA curve showed no sharp peak, while endothermic behavior was observed at temperatures ranging from room temperature to 550 °C. Therefore, the gradual decomposition of SEI occurs over a wide range of temperature. A mass signal of $m/z = 44$ appeared at temperatures between 200 and 500 °C. Therefore, the weight loss from 200 to 500 °C was attributed to the release of $CO_2$ which was caused by the decomposition of SEI.

The influence of the charging-depth on the thermal properties of SEI was investigated using graphite electrodes that had been cycled in potential ranges from 2.0 to 0.5, 0.1, 0.05 or 0.01 V. Since SEI on a graphite electrode can be formed by the reductive decomposition of electrolyte during the 1st charge, graphite test electrodes after the first charge/discharge cycle were used. Before the cell was disassembled, the electrode was kept at 2.0 V (discharged state) to reach a steady-state. Fig. 2 shows the variation of the mass signal of $m/z = 44$ with temperature

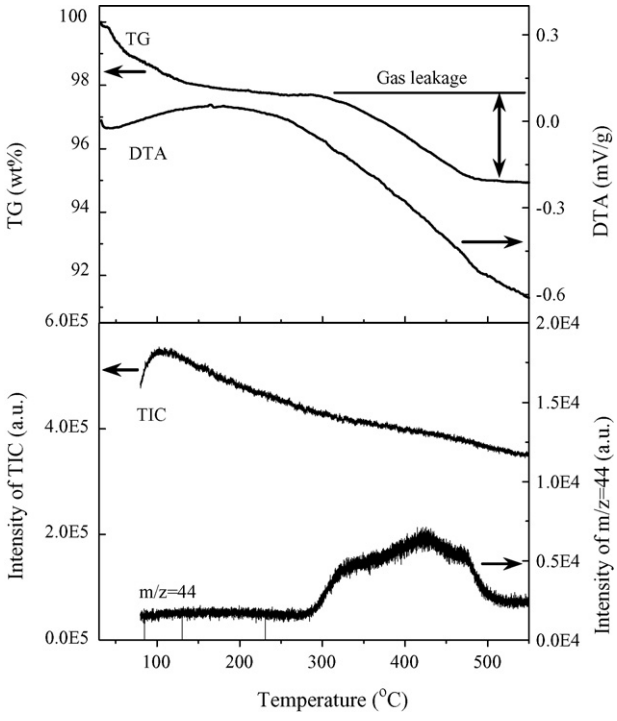


Fig. 1. TG/DTA/MS curves of sample powders in the discharged state after the second cycle.

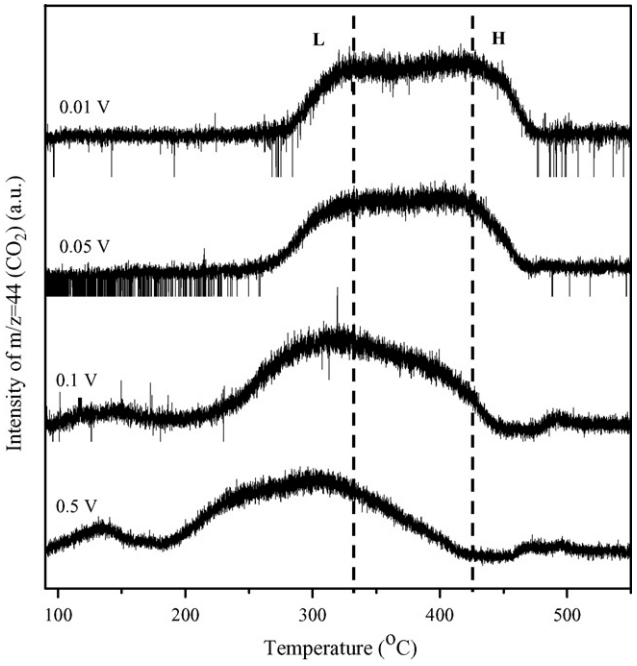


Fig. 2. Variation of the mass signal of $m/z = 44$ with temperature for sample powders in the discharged state after charging to 0.01, 0.05, 0.1 and 0.5 V.

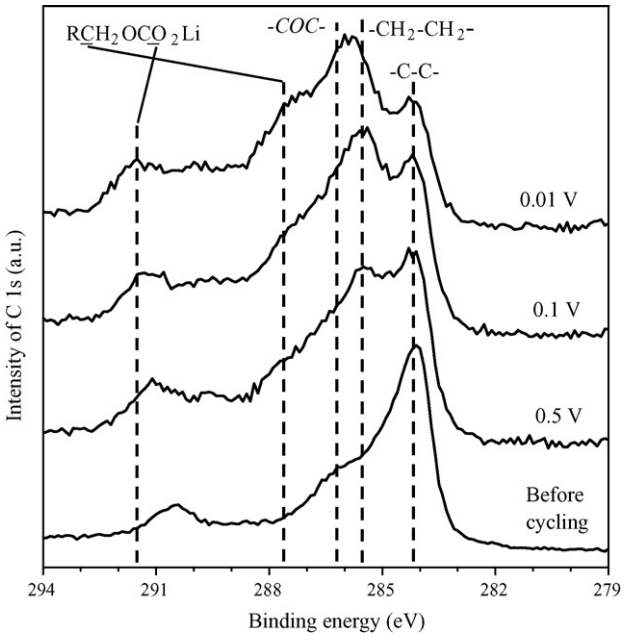


Fig. 3. C 1s spectra of graphite electrodes in the discharged state which was obtained after the 1st cycle within a potential range from 2.0 to 0.5, 0.1, or 0.01 V, together with that of the electrode before cycling as a reference.

for sample powders at a discharged state after being charged to 0.01, 0.05, 0.1 and 0.5 V. In addition to a continuous background, the sample that had been subjected to 0.5 V gave small peaks at around 130, 470 and 495 °C, and a broad peak between 190 and 410 °C. These results indicate that the SEI was thermally decomposed within a wide temperature-range from 100 to 500 °C. The small peak gradually disappeared with a decrease in the potential, while the broad peak became narrow and shifted toward a high temperature. The samples that had been subjected to 0.05 and 0.01 V gave two prominent peaks at around 330 and 430 °C. These results indicate that the SEI should consist of two dominant components, which were referred to as components L and H, respectively. Although no peak was seen at 430 °C for the sample that had been subjected to a high potential of 0.5 V, it increased with a decrease in potential. Therefore, component H seems to be formed at lower potential than component L.

The influence of the charging-depth on the chemical composition of the SEI was investigated by XPS. Fig. 3 shows C 1s spectra of graphite electrodes in the discharged state which was obtained after the 1st cycle between 2.0 and 0.5, 0.1, or 0.01 V, together with that of the electrode before cycling as a reference. Before cycling, a sharp peak at 284.2 eV, which is due to graphite, with a shoulder peak at higher binding energy was observed. The peak at 290.5 eV was assigned to the PVdF binder. After cycling, peaks at around 286, 287.6 and 291.5 eV appeared, indicating the formation of SEI. The peak at around 286 eV contained contributions from two subpeaks due to hydrocarbons (285.5 eV) and an oxygen-containing polymeric component (286.2 eV). The peaks at 291.5 and 287.6 eV were attributed to the carbon atoms of the carbonate group and alkyl group in the lithium alkyl carbonate ($RCH_2OCOOLi$), respectively. The intensity of these peaks increased with a decrease in the potential, while that of the peak at 284.2 eV due to graphite decreased. This result indicates that the test electrode was covered with SEI, and the thickness of the SEI increased at a deeper charging-depth. The intensity of the peaks at 291.5 and 287.6 eV was almost comparable for the electrode that had been subjected to 0.5 V, which indicates that the peaks reflected lithium alkyl carbonate. However, the peak intensity at 287.6 eV significantly increased with a decrease in potential compared to that at 291.5 eV. Therefore, other functional groups such as carbonyl and ester, which also give a peak at around 287.6 eV [11], may be formed at lower potentials. Thus, the composition of SEI was influenced by the charging-depth.

Fig. 4 shows TG-MS spectra of $m/z = 44$ for sample powders that had been cycled repeatedly between 0.01 and 2.0 V. The test electrode was kept at a discharged state to reach a steady state before the cell was disassembled. After the 1st cycle, $CO_2$ evolution was found at temperatures between 280 and 470 °C, which consisted of two peaks at around 330 and 430 °C, as shown in Fig. 2. The intensity of the former peak gradually decreased with an increase in the cycle number, while the latter remarkably increased. Only the peak at 430 °C due to component H was observed after the 50th cycle. It indicated that component L may be converted into component H. A similar tendency was seen in terms of charging-depth, as shown in Fig. 2.

Fig. 5 shows C 1s spectra of graphite electrodes after the 1st, 10th, and 50th cycles between 0.01 and 2.00 V. The peak at 284.2 eV due to graphite gradually faded with an increase in the cycle number, which indicates a gradual increase in the SEI thickness. In addition, a peak at 290.3 eV appeared after the 50th cycle, which suggests the appearance of lithium carbonate. Almost no peak was seen at 291.5 eV after the 50th cycle, while the peak at 287.6 eV was still observed. This result indicates that lithium alkyl carbonate should be converted to products with other functional groups, such as carbonyl and ester, over repeated

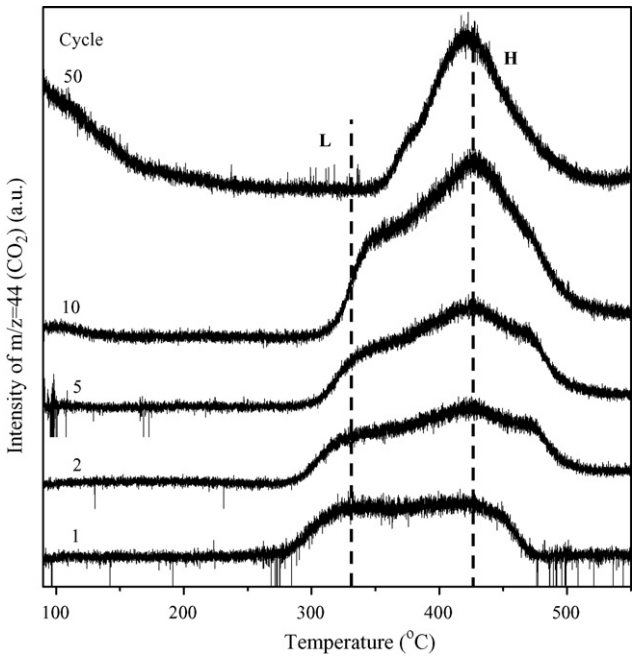


Fig. 4. Variation of the mass signal of $m/z = 44$ with temperature for sample powders in the discharged state after the 1st, 2nd, 5th, 10th and 50th cycles.

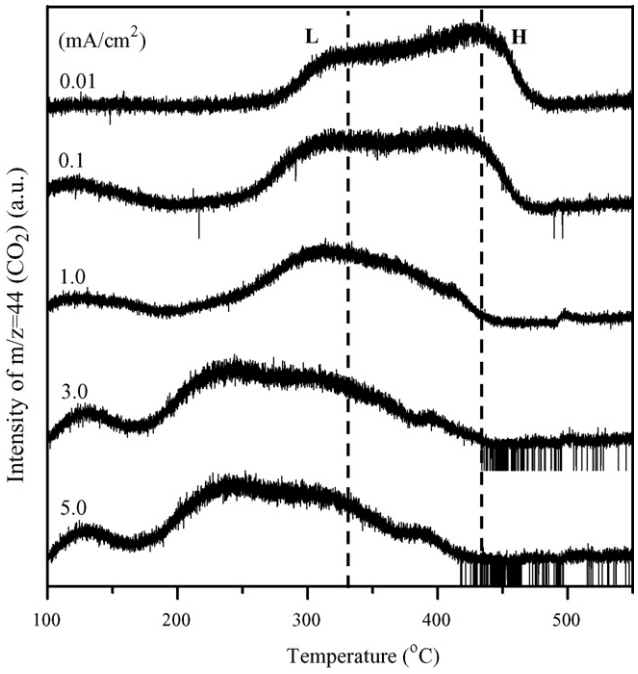


Fig. 6. Variation of the mass signal of $m/z = 44$ with temperature sample powders that had been cycled between 0.01 and 2.0 V at constant current densities of 0.01, 0.1, 1.0, 3.0 and 5.0 mA $cm^{-2}$ at 25 °C.

cycling, as discussed in Fig. 3. Based on the present results and by considering the finding that the peaks due to component L in the TG-MS curves disappeared after repeated cycling, component L could be identified as lithium alkyl carbonate. On the other hand, component H may be assigned to hydrocarbons, an oxygen-containing polymeric component, and/or other species containing a functional group of carbonyl or ester. This assumption is discussed below.

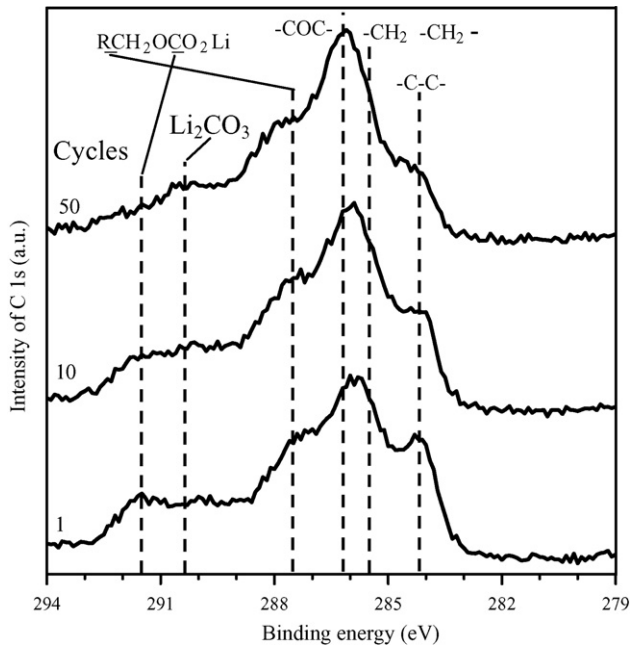


Fig. 5. C 1s spectra of graphite electrodes after the 1st, 10th and 50th cycles between 0.01 and 2.0 V.

The electrochemical properties of SEI are known to be influenced by the current density during the charge/discharge cycle [16,17]. Fig. 6 shows the variation of the mass signal of $m/z = 44$ with temperature for sample powders that had been cycled between 0.01 and 2.0 V at constant current densities of 0.01, 0.1, 1.0, 3.0 and 5.0 mA $cm^{-2}$ at 25 °C. While a broad peak was seen from 180 to 420 °C at 3.0 and 5.0 mA $cm^{-2}$, it shifted toward high temperature with a decrease in the current density. Two prominent peaks at 330 and 430 °C were seen at current densities below 0.1 mA $cm^{-2}$. Moreover, the peak at 430 °C increased with a decrease in the current density; the amount of component H increased compared to component L. At low current densities, considerable time is needed to achieve charge/discharge processes, and hence the test electrode should be subjected to low potentials for a long time. Therefore, component L seems to be reductively decomposed into component H. These results support the above discussion in Fig. 4.

Fig. 7 shows the variation of the mass signal of $m/z = 44$ with temperature for sample powders that had been cycled between 0.01 and 2.0 V at an elevated temperature of 60 °C. No obvious difference was observed between the curves, compared to those at 25 °C (Fig. 6); at temperatures from 180 to 270 °C, no broad peak was seen at current densities above 3.0 mA $cm^{-2}$. In addition, the peaks due to component H at 430 °C appeared even at current densities above 3.0 mA $cm^{-2}$. The present results indicate that component H could be easily formed at elevated temperature by the reductive decomposition of component L. Thus, reductive decomposition of the SEI components can be accelerated at elevated temperature.

Fig. 8 shows the variation of the mass signal of $m/z = 44$ with temperature for sample powders that had been charged at 0.1 V

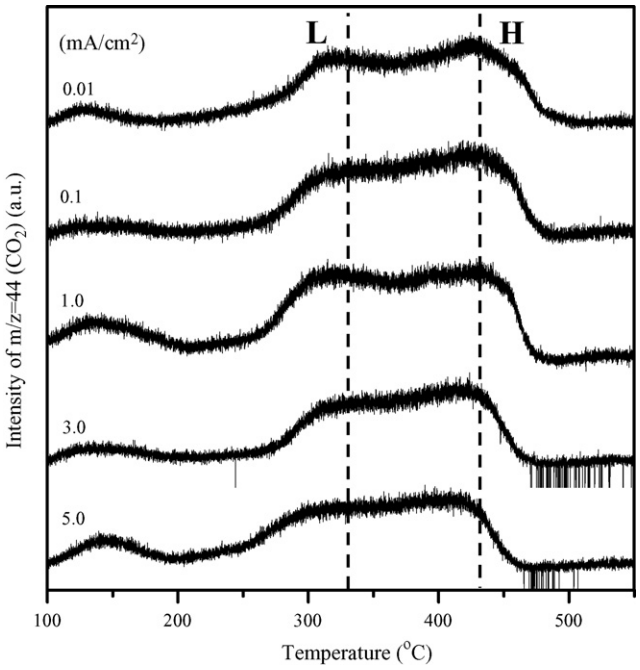


Fig. 7. Variation of the mass signal of $m/z = 44$ with temperature for sample powders that had been cycled between 0.01 and 2.0 V at constant current densities of 0.01, 0.1, 1.0, 3.0 and 5.0 mA $cm^{-2}$ at an elevated temperature of 60 °C.

or discharged at 2.0 V. A significant difference was seen between charged and discharged samples; discharged samples showed a broad peak from 230 to 440 °C, while charged samples gave a sharp peak at around 430 °C. The peak intensity at 430 °C due to component H increased after the 2nd cycle for discharged samples. A trend similar to that in Fig. 4 was seen. On the other hand, only the peak due to component H was observed for charged samples, and this seemed to be accompanied by the fading of component L. In addition, it is unlikely that the composition of the SEI changes during the charge and discharge cycles. Therefore, component L in the SEI of charged samples should be completely converted into component H at elevated temperatures during TG-MS measurements; since the charged graphite at 0.1 V is highly reducible, component L seems to be reductively decomposed into component H. Based on these results, component H can be formed by the reductive decomposition of lithium alkyl carbonate.

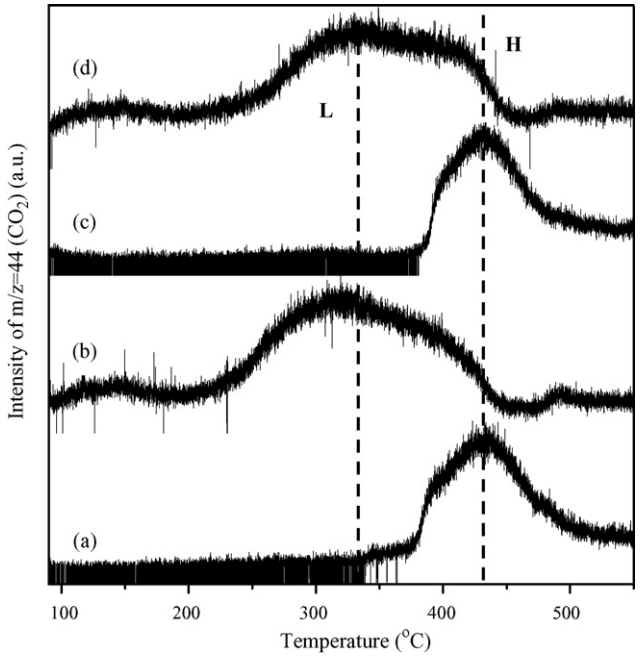


Fig. 8. Variation of mass signal of $m/z = 44$ with temperature for sample powders that had been (a) charged at 0.1 V during the 1st cycle, (b) discharged at 2.0 V after the 1st cycle, (c) charged at 0.1 V during the 2nd cycle, and (d) discharged at 2.0 V after the 2nd cycle.

Zhuang and Ross [9,18] reported that lithium oxalate ($Li_2C_2O_4$) was an important component in SEI and might be formed by the decomposition of lithium alkyl carbonate. Hence, component H may be attributed to lithium oxalate. This assumption was examined by TG-MS and XPS measurements of a commercial lithium oxalate sample with 95% purity. TG-MS curves of lithium oxalate showed $CO_2$ evolution at about 400 °C, which is in good agreement with the temperature for the decomposition of component H, as shown in Figs. 2, 4 and 7. On the other hand, with graphite C 1s peak of 284.2 eV as an internal standard to calibrate the binding energy scale, lithium oxalate showed a C 1s peak at 287.6 eV in XPS spectrum. This result agrees well with that of component H in Figs. 3 and 5. Furthermore, an oxalate functional group was reported to show a C 1s peak at 288 eV in XPS spectrum [19], which also supports our assumption. Consequently, component H was mainly considered to be lithium oxalate.

Based on the above results and discussion, SEI contains lithium oxalate, in addition to lithium alkyl carbonate, hydrocarbons, oxygen-containing polymeric species, and lithium carbonate. Thus, the chemical composition of SEI was not homogeneous. The formation of lithium oxalate was accompanied by a decrease in lithium alkyl carbonate and was slower than that of lithium alkyl carbonate; the amount of lithium oxalate increased with an increase in the charging depth and also with an increase in the cycle number. Hence, lithium oxalate seems to be formed by the reductive decomposition of lithium alkyl carbonate during charge and discharge processes. In EC + DMC-based electrolyte, EC and DMC are reductively decomposed to form lithium ethylene dicarbonate ($LiO_2COCH_2CH_2OCO_2Li$) and lithium methyl carbonate ($CH_3OCO_2Li$), respectively [7]. Based on reports in literature, the following mechanism can be proposed for the formation of lithium oxalate in SEI [20]:

$$(CH_2OCO_2Li)_2 + 2e^- + 2Li^+ \rightarrow (COOLi)_2 + (CH_2OLi)_2$$

$$2CH_3OCO_2Li + 2e^- + 2Li^+ \rightarrow (COOLi)_2 + 2CH_3OLi$$

By considering the results in Fig. 8, the above reactions were accelerated by charged graphite electrodes; lithium alkyl carbonate in SEI can be easily reduced by intercalated lithium-ion in graphite, which results in the formation of lithium oxalate.

## 4. Conclusions

The thermal properties and chemical components of SEI formed on a graphite electrode were investigated by TG-

DTA/MS and XPS. SEI on the graphite electrode in the discharged state was decomposed at temperatures of around 330 and 430 °C and was accompanied by $CO_2$ evolution. However, while $CO_2$ evolution at 330 °C was not seen after prolonged charge/discharge cycles, that at 430 °C increased. These results indicate the component that can be decomposed at 330 °C was reductively decomposed into that at 430 °C. Based on these results and by considering the C1s spectra of SEI, $CO_2$ evolution at 330 and 430 °C is considered to be mainly caused by the decomposition of lithium alkyl carbonate and lithium oxalate, respectively. It was found that lithium oxalate was reduction product of lithium alkyl carbonate during the intercalation of lithium ions. The reduction reaction could be accelerated by elevated temperature. The transformation of SEI chemical structure showed direct effect on the thermal stability of SEI. At the same time, lithium carbonate was also found in SEI on the graphite electrode after long cycles, while it was negligible in the electrode subjected to short cycles.

## Acknowledgement

This work was supported in part by CREST of Japan Science and Technology (JST) Corporation.

## References

[1] P. Novák, F. Joho, M. Lanz, B. Rykart, J.-C. Panitz, D. Alliata, R. Kötz, O. Haas, J. Power Sources 97–98 (2001) 39–46.
[2] Y. Ein-Eli, Electrochem. Solid State Lett. 2 (1999) 212–214.
[3] E. Peled, D. Golodnitsky, C. Menachem, D. Bar-Tow, J. Electrochem. Soc. 145 (1998) 3482–3486.
[4] D. Aurbach, B. Markovsky, A. Shechter, Y. Ein-Eli, H. Cohen, J. Electrochem. Soc. 143 (1996) 3809–3820.
[5] D. Aurbach, M.D. Levi, E. Levi, A. Schechter, J. Phys. Chem. B 101 (1997) 2195–2206.
[6] E. Peled, D. Golodnitsky, A. Ulus, V. Yufit, Electrochim. Acta 50 (2004) 391–395.
[7] D. Aurbach, E. Zinigrad, Y. Cohen, H. Teller, Solid State Ionics 148 (2002) 405–416.
[8] E. Peled, D.B. Tow, A. Merson, A. Gladkich, L. Burstein, D. Golodnitsky, J. Power Sources 97–98 (2001) 52–57.
[9] G.V. Zhuang, P.N. Ross, Electrochem. Solid State Lett. 6 (2003) A136–A139.
[10] S.S. Zhang, K. Xu, T.R. Jow, Electrochim. Acta 51 (2006) 1636–1640.
[11] M. Herstedt, A.M. Andersson, H. Rensmo, H. Siegbahn, K. Edström, Electrochim. Acta 49 (2004) 4939–4947.
[12] M. Herstedt, D.P. Abraham, J.B. Kerr, K. Edström, Electrochim. Acta 49 (2004) 5097–5110.
[13] C.R. Yang, Y.Y. Wang, C.C. Wan, J. Power Sources 72 (1998) 66–70.
[14] D. Aurbach, B. Markovsky, I. Weissman, E. Levi, Y. Ein-Eli, Electrochim. Acta 45 (1999) 67–86.
[15] D. Zane, A. Antonini, M. Pasquali, J. Power Sources 97–98 (2001) 146–150.
[16] M. Dollé, S. Grugeon, B. Beaudoin, L. Dupont, J.-M. Tarascon, J. Power Sources 97–98 (2001) 104–106.
[17] H. Ota, T. Sato, H. Suzuki, T. Usami, J. Power Sources 97–98 (2001) 107–113.
[18] C.-M. Lee, B.-J. Mun, P.N. Ross, J. Electrochem. Soc. 149 (2002) A1286–A1292.
[19] D. Banerjee, H.W. Nesbitt, Geochim. Cosmochim. Acta 63 (1999) 3025–3038.
[20] G.V. Zhuang, H. Yang, B. Blizanac, P.N. Ross, Electrochem. Solid State Lett. 8 (2005) A441–A445.